4-2015

# Effects of Cannabidiol on Contractions and Calcium Signaling in Rat Ventricular Myocytes

Ramez M. Ali
*UAE University, Al Ain, Abu Dhabi, UAE*

Lina T. Al Kury
*UAE University, Al Ain, Abu Dhabi, UAE*

Keun-Hang Susan Yang
*Chapman University*, kyang@chapman.edu

Anwar Qureshi
*UAE University, Al Ain, Abu Dhabi, UAE*

Mohanraj Rajesh
*UAE University, Al Ain, Abu Dhabi, UAE*

***See next page for additional authors***



Recommended Citation
R.M. Ali, L.T.A. Kury, K.-H.S. Yang, A. Qureshi, M. Rajesh, S. Galadari, Y.M. Shuba, F.C. Howarth, M. Oz, Effects of cannabidiol on contractions and calcium signaling in rat ventricular myocytes, *Cell Calcium* (2015), http://dx.doi.org/10.1016/j.ceca.2015.02.001

# Effects of Cannabidiol on Contractions and Calcium Signaling in Rat Ventricular Myocytes





**Authors**
Ramez M. Ali, Lina T. Al Kury, Keun-Hang Susan Yang, Anwar Qureshi, Mohanraj Rajesh, Sehamuddin Galadari, Yaroslav M. Shuba, Frank Christopher Howarth, and Murat Oz

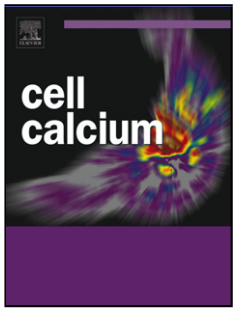


Title: Effects of cannabidiol on contractions and calcium signaling in rat ventricular myocytes

Author: Ramez M. Ali Lina T. Al Kury Keun-Hang Susan Yang Anwar Qureshi Mohanraj Rajesh Sehamuddin Galadari Yaroslav M. Shuba Frank Christopher Howarth Murat Oz

PII: S0143-4160(15)00033-0
DOI: http://dx.doi.org/doi:10.1016/j.ceca.2015.02.001
Reference: YCECA 1653

To appear in: *Cell Calcium*

Received date: 24-11-2014
Revised date: 20-1-2015
Accepted date: 2-2-2015

Please cite this article as: R.M. Ali, L.T.A. Kury, K.-H.S. Yang, A. Qureshi, M. Rajesh, S. Galadari, Y.M. Shuba, F.C. Howarth, M. Oz, Effects of cannabidiol on contractions and calcium signaling in rat ventricular myocytes, *Cell Calcium* (2015), http://dx.doi.org/10.1016/j.ceca.2015.02.001

**Effects of cannabidiol on contractions and calcium signaling in rat ventricular myocytes.**

Ramez M. Ali[1], Lina T. Al Kury[1], Keun-Hang Susan Yang[5], Anwar Qureshi[2], Mohanraj Rajesh[1], Sehamuddin Galadari[3], Yaroslav M. Shuba[4], Frank Christopher Howarth[2], Murat Oz[1].

[1]Laboratory of Functional Lipidomics, Department of Pharmacology, [2]Department of Physiology, [3]Department of Biochemistry, College of Medicine and Health Sciences, UAE University, Al Ain, Abu Dhabi, UAE, [4]Bogomoletz Institute of Physiology and International Center of Molecular Physiology, National Academy of Sciences of Ukraine, Kyiv-24, Ukraine, [5]Department of Biological Sciences, Schmid College of Science and Engineering, Chapman University, One University Drive, Orange, CA 92866, USA.

Address for correspondence:

Dr. Murat Oz,

Department of Pharmacology and Therapeutics,

College of Medicine & Health Sciences,

UAE University; P.O. Box 17666

Al Ain, Abu Dhabi, UAE

Phone: 00 971 3 7137523

Fax: 00 971 3 7672033

E-mail: murat_oz@uaeu.ac.ae

**Abstract**

Cannabidiol (CBD), a major nonpsychotropic cannabinoid found in *Cannabis* plant, has been shown to influence cardiovascular functions under various physiological and pathological conditions. In the present study, the effects of CBD on contractility and electrophysiological properties of rat ventricular myocytes were investigated. Video edge detection was used to measure myocyte shortening. Intracellular $Ca^{2+}$ was measured in cells loaded with the $Ca^{2+}$ sensitive fluorescent indicator fura-2 AM. Whole-cell patch clamp was used to measure action potential and $Ca^{2+}$ currents. Radioligand binding was employed to study pharmacological characteristics of CBD binding. CBD (1 μM) caused a significant decrease in the amplitudes of electrically-evoked myocyte shortening and $Ca^{2+}$ transients. However, the amplitudes of caffeine-evoked $Ca^{2+}$ transients and the rate of recovery of electrically-evoked $Ca^{2+}$ transients following caffeine application were not altered. Whole-cell patch-clamp technique was employed to investigate the effect of CBD on the characteristics of action potentials (APs) and L-type $Ca^{2+}$ channels. CBD (1 μM) significantly decreased the duration of APs. Further studies on L-type $Ca^{2+}$ channels indicated that CBD inhibits these channels with $IC_{50}$ of 0.1 μM in a voltage-independent manner. Radioligand studies indicated that the specific binding of [$^3$H]Isradipine, was not altered significantly by CBD. The results suggest that CBD depresses myocyte contractility by suppressing L-type $Ca^{2+}$ channels at a site different than dihydropyridine binding site and inhibits excitation-contraction coupling in cardiomyocytes.

**Key words:** Cannabidiol; Cannabinoid; Ventricular myocytes; Contraction; Intracellular calcium; Calcium channels.

**List of abbreviations:** Action potential (AP); Action potential duration (APD); Action potential duration at 60% level of repolarization ($APD_{60}$); Amplitude (AMP); Bovine serum albumin (BSA); Cannabidiol (CBD); $\Delta^9$-tetrahydrocannabinoid (THC); Dimethylsulphoxide (DMSO); Normal Tyrode (NT); Resting cell length (RCL); Sarcoplasmic reticulum (SR); Time from peak to half ($T_{HALF}$); Time to peak (TPK); Transient receptor potential (TRP).

**Running title:** cannabidiol on excitation-contraction

**Running head:** Effects of cannabidiol on rat ventricular myocytes

**Introduction**

Cannabidiol (CBD) is a major nonpsychoactive phytocannabinoid found in *Cannabis sativa*. Although it is devoid of psychoactive properties, in earlier studies CBD has been shown to possess anti-apoptotic, anti-oxidant, and anti-inflammatory effects [for reviews, 1, 2]. Interestingly, CBD displays low affinity for the cannabinoid $CB_1$ and $CB_2$ receptors [for reviews, 3, 4]. Thus, pharmacological actions of CBD have been suggested to be mediated mainly by its direct actions on various enzymes and ion channels or through a novel cannabinoid (non-$CB_1$ and non-$CB_2$) receptor [for reviews, 3, 4].

Several earlier studies indicate that CBD has beneficial effects in various cardiovascular pathologies such as myocardial infarction, ischemia-induced arrhythmias, and diabetic cardiomyopathy [5, 6, 7, 8]. Although anti-oxidant and anti-inflammatory actions have been suggested to be involved in these beneficial effects [9], the exact mechanisms of CBD actions are currently unknown.

Haeomodynamic effects of CBD have been investigated in earlier *in vivo* and *in vitro* studies [10]. In pentobarbitone anaesthetized rats, CBD has been shown to cause a significant but transient fall in mean arterial blood pressure [6]. Similarly, in arterial segments taken from rat mesenteric vascular bed that have been pre-constricted with phenylephrine, CBD has been shown to cause a concentration-dependent vasorelaxation [11]. Likewise, in rat isolated aortae, application of CBD (1-30 μM) caused vasorelaxation. In agreement with these findings, in human mesenteric arteries, it has been shown that CBD causes vasorelaxation of endothelin-1 pre-constricted arterial segments [12]. In these studies, both cannabinoid receptor-dependent and independent mechanisms have been shown to play roles in CBD inhibition of smooth muscle contraction. Further contributions to the complexity of CBD actions include the type of vascular structure, the presence of intact endothelium, the metabolic products of

endocannabinoids [13] and the activity of metabolizing enzymes have also been shown to modulate the actions of CBD on cardiovascular system [10].

Compared with the information available on the vascular effects of CBD, to our knowledge, there have been few studies focusing on the role of CBD in the regulation of contractility and $Ca^{2+}$ signaling in cardiac muscle. In earlier *in vitro* studies, negative inotropic and bradycardic effects of CBD have been reported [14]. In addition, in perfused rat heart, CBD has been shown to antagonize the $\Delta^9$-tetrahydrocannabinoid-induced positive inotropic effect and tachycardia, one of the most consistent cardiovascular effects of *Cannabis* intoxication [15]. In the present study, we have hypothesized that the negative inotropic actions of CBD observed in earlier studies are due to the inhibition of excitation-contraction coupling in ventricular myocytes. Thus, we have investigated the effects of CBD on contractility and electrical properties of acutely dissociated rat ventricular myocytes.

## Materials and Methods

*Ventricular myocyte isolation*

Ventricular myocytes were isolated from adult male Wistar rats (248 ± 17 g) according to previously described techniques [16]. This study was carried out in accordance with the recommendations in the Guide for the Care and Use of Laboratory Animals of the National Institutes of Health. The protocol was approved by the Committee on the Ethics of Animal Experiments of the UAE University. Briefly, the animals were euthanized using a guillotine and hearts were removed rapidly and mounted for retrograde perfusion according to the Langendorff method. Hearts were perfused at a constant flow of 8 ml g heart$^{-1}$ min$^{-1}$ and at 36-37 ˚C with a solution containing (mM): 130 NaCl, 5.4 KCl, 1.4 $MgCl_2$, 0.75 $CaCl_2$, 0.4 $NaH_2PO_4$, 5 HEPES, 10 glucose, 20 taurine, and 10 creatine set to pH 7.3 with NaOH. When the heart had stabilized, perfusion was continued for 4 min with $Ca^{2+}$-free isolation solution containing 0.1 mM EGTA, and then for 6 min with cell isolation solution containing 0.05 mM $Ca^{2+}$, 0.75 mg/ml collagenase (type 1; Worthington Biochemical Corp, USA) and 0.075 mg/ml protease (type X1 V; Sigma, Germany). Ventricles were excised from the heart, minced and gently shaken in collagenase-containing isolation solution supplemented with 1 % BSA. Cells were filtered from this solution at 4 minute intervals and resuspended in isolation solution containing 0.75 mM $Ca^{2+}$.

*Measurement of ventricular myocyte shortening*

Ventricular myocytes were allowed to settle on the glass bottom of a Perspex chamber mounted on the stage of an inverted microscope (Axiovert 35, Zeiss, Germany). Myocytes were superfused (3–5 ml/min) with normal Tyrode (NT) containing (mM): 140 NaCl, 5 KCl, 1 $MgCl_2$, 10 glucose, 5 HEPES, 1.8 $CaCl_2$ (pH 7.4). Shortening of myocytes was recorded using a video edge detection system (VED-

114, Crystal Biotech, USA). Resting cell length (RCL) and amplitude of shortening (expressed as a % of resting cell length) were measured in electrically stimulated (1 Hz) myocytes maintained at 35–36˚C. Data were acquired and analyzed with Signal Averager software v 6.37 (Cambridge Electronic Design, UK). Experimental solutions were prepared from stocks immediately prior to each experiment.

*Measurement of intracellular $Ca^{2+}$ concentration*

Myocytes were loaded with the fluorescent indicator fura-2 AM (F-1221, Molecular Probes, USA) as described previously [17]. In brief, 6.25 µl of a 1 mM stock solution of fura-2 AM (dissolved in dimethylsulphoxide) was added to 2.5 ml of cells to give a final fura-2 concentration of 2.5 µM. Myocytes were shaken gently for 10 min at 24 ˚C (room temperature). After loading, myocytes were centrifuged, washed with NT to remove extracellular fura-2 and then left for 30 min to ensure complete hydrolysis of the intracellular ester. To measure intracellular $Ca^{2+}$concentration, myocytes were alternately illuminated by 340 and 380 nm light using a monochromator (Cairn Research, UK) which changed the excitation light every 2 ms. The resulting fluorescence emitted at 510 nm was recorded by a photomultiplier tube and the ratio of the emitted fluorescence at the two excitation wavelengths (340/380 ratio) was calculated to provide an index of intracellular $Ca^{2+}$ concentration. Resting fura-2 ratio, TPK $Ca^{2+}$ transient, $T_{HALF}$ decay of the $Ca^{2+}$ transient, and the amplitude of the $Ca^{2+}$ transient were measured in electrically stimulated (1 Hz) myocytes.

*Measurements of sarcoplasmic reticulum $Ca^{2+}$ content*

Sarcoplasmic reticulum (SR) $Ca^{2+}$ release was assessed using previously described techniques [18]. After establishing steady state $Ca^{2+}$ transients in electrically stimulated (1 Hz) myocytes maintained at 35– 36 ˚C and loaded with fura-2, stimulation was paused for a period of 5 s. Caffeine (20 mM) was then applied for 10 s using a solution switching device customized for rapid solution

exchange. Electrical stimulation was resumed and the $Ca^{2+}$ transients were allowed to recover to steady state. SR- releasable $Ca^{2+}$ was assessed by measuring the area under the curve of the caffeine-evoked $Ca^{2+}$ transient. Fractional release of SR $Ca^{2+}$ was assessed by comparing the amplitude of the electrically evoked steady state $Ca^{2+}$ transients with that of the caffeine-evoked $Ca^{2+}$ transient and refilling of SR was assessed by measuring the rate of recovery of electrically evoked $Ca^{2+}$ transients following application of caffeine.

*Assessment of myofilament sensitivity to $Ca^{2+}$*

In some cells shortening and fura-2 ratio were recorded simultaneously. Myofilament sensitivity to $Ca^{2+}$ was assessed from phase-plane diagrams of fura-2 ratio vs. cell length by measuring the gradient of the fura-2-cell length trajectory during late relaxation of the twitch contraction. The position of the trajectory reflects the relative myofilament response to $Ca^{2+}$ and hence, was used as a measure of myofilament sensitivity to $Ca^{2+}$ [19].

*Electrophysiological measurements of action potentials*

Action potentials (APs) were measured using whole-cell patch clamp technique. Recordings were made with an Axopatch 200B amplifier (Molecular Devices, Downington, PA, USA) coupled to an A/D interface (Digidata 1322; Molecular Devices, Downington, PA, USA). Patch pipettes were fabricated from filamented GC150TF borosilicate glass (Harvard Apparatus, Holliston, MA, USA) on a horizontal puller (Sutter Instruments Co., Novato, CA). Electrode resistances ranged from 2.0 to 3.0 MΩ, and seal resistances were 1-5 GΩ. After giga seal formation, the membrane was ruptured with gentle suction to obtain whole cell current-clamp configuration. APs were elicited by injection of 0.9 to 1 nA square current pulses for 4-ms at a frequency of 0.2 Hz. Extracellular solution contained (mM): 144 NaCl, 5.4 KCl, 1.8 $CaCl_2$, 1.2 $MgCl_2$, 1 $NaH_2PO_4$, 10 HEPES, 10 glucose, and pH 7.4 (adjusted

with NaOH). Recording pipettes were filled with intracellular solution containing (mM): 150 KCl, 10 NaCl, 120 aspartate, 5 $MgCl_2$, 0.1 $CaCl_2$, 1.1 EGTA, 10 HEPES, 4 Mg-ATP, 5 sucrose, and pH 7.2 (adjusted with HCl). Experiments were performed at room temperature (22-24 ºC). Changes of external solutions and application of drugs were performed using a multi-line perfusion system driven by a micro-pump with a common outflow connected to the cell chamber. In some experiments, applications of drugs were performed using multi-barrel puffing micropipette with a common outflow positioned in close proximity to the cell under investigation. Complete external solution exchange was achieved in <1 s. In recording of $Ca^{2+}$ currents, voltage pulses were elicited from a holding potential of −50 mV to membrane potentials ranging from -70 mV to +70 mV in 10 mV increments every 300 ms. The whole-cell bath solution contained (mM): 95 NaCl, 50 TEACl, 2 $MgCl_2$, 2 $CaCl_2$, 10 HEPES and 10 glucose (adjusted to pH 7.35 with NaOH). The pipette solution contained (mM): 140 CsCl, 10 TEACl, 2.0 $MgCl_2$, 2 HEPES 1 MgATP and 10 EGTA (adjusted to pH 7.25 with CsOH).

*Radioligand binding studies with [$^3$H]Isradipine*

Experiments on the binding of [$^3$H]Isradipine (Specific activity 58.6 Ci /mmol, New England Nuclear, Chadds Ford, PA, USA) were conducted similar to our earlier studies [20]. Briefly, aliquots of membranes (0.1 mg) were added to different concentrations of radiolabeled ligand to give a final concentration of 0.02 mg/ml membranes in a total volume of 0.8 ml. After 60 min incubation at room temperature, 0.4 ml aliquots of each sample were filtered under vacuum through Watman GF\C filters and rapidly washed with 5 ml of ice-cold assay buffer. The filters were dried and extracted in 5 ml of Hydroflour™ (National Diagnostics, St. Louis, MO, USA) scintillation fluid before counting for $^3$H. Triplicate 50-µl samples of the incubation mixtures were also counted directly for estimations of total binding. Nonspecific binding was estimated from parallel measurements of binding in the presence of 5

μM unlabeled nifedipine. DMSO, at the highest concentration used in our experiments (0.02 % v/v) had no effect on the specific binding of [$^3$H]Isradipine.

Cannabidiol (purchased from Ascent Scientific, Cambridge, UK) was dissolved in DMSO. In our control experiments, DMSO, at the highest concentration used (0.02 % v/v), caused 18-20 % inhibition of the shortening in experiments lasting up to 20-25 min. Stock solutions of CBD were kept at -20 °C until its use. Reagents and chemicals used in our experiments were purchased from Sigma-Aldrich (St. Louis, MO, USA). Stocks were kept at -20 °C until their use.

*Data Analysis*

Electrophysiological data were analyzed using pClamp 8.0 (Molecular Devices, Downington, PA), Origin 8.0 (Origin Lab Corp., Northampton, MA) and Mat Lab R2011a (MathWorks Corp., Natick, MA) software. APD was measured at 60 % of repolarization from AP amplitude. The results of the experiments were expressed as mean ± standard error of the mean (S.E.M.). Statistical analysis was performed using the paired *t*-test (within the same cell analysis). Statistical significance among groups was determined using one way ANOVA followed by Bonferroni Post-hoc analysis. Statistical analysis of the data was performed using Origin 7.0 software (OriginLab Corp., Northampton, MA) and IBM SPSS statistics version 20. On all graphs (*) denotes statistical significance with $P<0.05$, between specified values, or if not specified to the respective control.

**Results**

*Effects of cannabidiol on ventricular myocyte shortening*

In Normal Tyrode (NT) solutions, amplitudes of myocyte shortening in response to electrical stimulation (stimulated at 1 Hz) gradually decreased to 85-80 % of controls during experiments lasting up to 20 min. No further run down of the shortening amplitudes was observed in NT solution containing 0.02 % DMSO (used as vehicle in 1 μM CBD solution; data not shown; n=11; compared to 0 time point; ANOVA, $P>0.05$) and, unless it was stated otherwise, DMSO (in the concentration used in CBD containing solution) was also included routinely in control (NT) solutions during shortening and $Ca^{2+}$ transient experiments.

Fig. 1A shows typical records of shortening in a myocyte superfused with either NT (in the absence of CBD, NT contained 0.02 % DMSO in all experiments) or NT + 1 μM CBD and during washout with NT. Time course of the effect of CBD was presented in the Fig. 1B. The effect of CBD reached a steady level within 5 min of CBD application. Increasing the incubation time to 10 min did not cause further change in the amplitudes of shortening. Recovery from CBD inhibition was incomplete during the 5-10 min washout time. In summary, the amplitude of shortening measured after 5 min bath application of CBD was significantly (paired *t*-test; n=17; $P<0.05$) reduced up to 46.4 ± 3.1 % of controls (Fig.1C). Concentration-response relationship normalized to maximal CBD inhibition indicated that CBD suppresses shortening of amplitudes with an $IC_{50}$ of 0.6 μM (Fig. 1D).

*Effects of cannabidiol on intracellular $Ca^{2+}$ levels*

We have investigated the effects of 5 min bath application of 1 μM CBD on the resting intracellular $Ca^{2+}$ levels and on the amplitudes and kinetics of $Ca^{2+}$ transients elicited by electrical-field stimulation. Typical records of $Ca^{2+}$ transients in a myocyte superfused with NT (containing 0.02 % DMSO), NT + 1 μM CBD and during washout with NT are shown in Fig. 2A. The effects of 1 μM CBD on resting fura-2 ratio, TPK $Ca^{2+}$ transients, $T_{HALF}$ decay of the $Ca^{2+}$ transients, and AMP of $Ca^{2+}$ transients are shown in Fig. 2B-E, respectively. Although, CBD has been shown to alter intracellular $Ca^{2+}$ levels in various types of cells [for reviews, 3, 9], application of 1 μM CBD for 5 to10 min did not cause a significant alteration in resting fura-2 ratio, TPK $Ca^{2+}$ transients, and $T_{HALF}$ decay of the $Ca^{2+}$ transients (paired *t*-test; n=11-14 cells, $P>0.05$). However, AMP of the $Ca^{2+}$ transients were significantly reduced by 1 μM CBD (0.337 ± 0.043 fura-2 ratio units) compared to 0.488 ± 0.056 fura-2 ratio units (paired *t*-test, n =11 cells) in controls.

*Effects of cannabidiol on sarcoplasmic reticulum $Ca^{2+}$ transport*

Maximal amplitudes and the rates of $Ca^{2+}$ release by 20 mM caffeine remained unaltered after 10 min bath application of 1 μM CBD (Figure 3A and 3B; paired *t*-test; n = 7 cells, $P>0.05$).

Fig. 3C shows a typical record illustrating the protocol used to measure fractional release of SR $Ca^{2+}$. Initially, the myocyte was electrically stimulated at 1Hz. Electrical stimulation was then turned off for 5 s. Caffeine was then applied for 10 s using a rapid solution-exchanger device. Electrical stimulation was then restarted, and the recovery of intracellular $Ca^{2+}$ was recorded during a period of 60 s. SR $Ca^{2+}$ content was assessed by measuring caffeine-evoked $Ca^{2+}$ release (area under the caffeine-evoked $Ca^{2+}$ transient) and fractional release of $Ca^{2+}$ by comparing the amplitude of the electrically evoked steady-state $Ca^{2+}$ transients with that of the caffeine-evoked $Ca^{2+}$ transient in the presence of

either NT alone or NT with 1 μM CBD. Fractional release of SR $Ca^{2+}$ was not significantly altered in 1 μM CBD compared to NT (0.78 ± 0.04 in CBD versus 0.81 ± 0.07 in controls; paired *t*-test; n =8 cells; Fig. 3D). The recovery of the $Ca^{2+}$ transients during electrical stimulation following application of caffeine (Fig. 3D) was also not significantly altered in myocytes exposed to 1 μM CBD myocytes compared to control cells (paired *t*-test; n = 8 cells, $P>0.05$).

*Effects of cannabidiol on myofilament sensitivity to $Ca^{2+}$*

The effects of CBD on myofilament sensitivity to $Ca^{2+}$ were also investigated. These experiments tested whether CBD decreases the mechanical responses by altering the affinity of the contractile machinery of the ventricular myocytes to intracellular $Ca^{2+}$. Typical record of myocyte shortening, fura-2 ratio and phase-plane diagrams of fura-2 ratio vs. cell length in myocytes exposed to NT are shown in Fig. 4A. The gradient of the trajectory reflects the relative myofilament response to $Ca^{2+}$ and hence, has been used as a measure of myofilament sensitivity to $Ca^{2+}$ [19]. The gradients of the fura-2-cell length trajectory during late relaxation of the twitch contraction measured during the periods 500-600 ms (Fig. 4B), 500-700 ms (Fig. 4C), and 500–800 ms (Fig. 4D) were not significantly altered in CBD compared to NT suggesting that myofilament sensitivity to $Ca^{2+}$ is not reduced by CBD (CBD-treatment was compared to NT containing 0.02 % DMSO, paired *t*-test; n = 17 cells; $P>0.05$).

*Effects of cannabidiol on the action potentials of ventricular myocytes*

In this set of experiments, patch-clamped cardiomyocytes were exposed to the CBD while continuously monitoring their $V_{rest}$ and APs in the current clamp mode. The generation of APs was evoked by 0.9-1 nA depolarizing current pulses of 4 ms duration. Since the intracellular pipette solution did not contain $Ca^{2+}$-chelating agents, the generation of each AP was accompanied by myocyte contraction. Therefore, current pulses were applied at a frequency of 0.2 Hz. During a typical

experiment following protocols were employed: first, whole-cell configuration was established and 4 to 5 min dialysis of the myocytes with pipette solution was allowed to ensure the equilibrium conditions between the intracellular pipette solution and intracellular milieu. After achieving stable recordings of baseline electrical activity ($V_{rest}$ and AP parameters), myocytes were exposed to CBD for 5 to 10 min and subsequently it was washed out.

Resting membrane potentials (means ± SEM) were -77.4 ± 1.9 and -79.2 ± 1.7 mV in control and after CBD treatment (n=9) myocytes, respectively (Fig. 5A, inset and Fig. 5B). Maximal amplitudes of AP and rate of rising of AP (maximal velocity; V/s, Fig. 5C and Fig 5D) were not altered significantly in the presence of CBD. CBD (1 μM) consistently shortened the duration of AP (measured at 60 % of repolarization, $APD_{60}$) (Figs. 5A inset and Fig. 5E). Changes in AP shortening in response to CBD (1 μM) application were noticeable within 20 to 30 s (*inset* to Fig. 5A). Recoveries were usually partial and required longer time.

*Effects of cannabidiol on L-type $Ca^{2+}$ currents*

We have also investigated the effect of CBD (1 μM) on the L-type $Ca^{2+}$ currents ($I_{L,Ca}$). Figure 6A shows a typical record of $I_{L,Ca}$ elicited by applying a single 300 ms voltage pulse to +10 mV from a holding potential of -50 mV in rat ventricular myocyte before and after 10 min superfusion with 1 μM CBD. Time course of the effect of CBD on the density of $I_{L,Ca}$ was presented in Figure 6B. Application of vehicle (0.02% DMSO) for 10 min caused a 10-15% inhibition of the current density of $I_{L,Ca}$ in experiments lasting up to 15 to 20 min. The effects of CBD were also investigated on the biophysical properties of $I_{L,Ca}$ in rat ventricular myocytes. $I_{L,Ca}$ was recorded in the presence of intracellular $Cs^+$ and extracellular $TEA^+$ to suppress $K^+$ currents while retaining 95 mM $Na^+$ in the extracellular solution. Elimination of contaminating $Na^+$ current during recording of $I_{L,Ca}$ was achieved by applying voltage step-pulses from relatively depolarized $V_h$ of -50 mV, which produced steady-state inactivation of sodium channels [21]. As evident from original recordings and *I-V* relationships (Fig. C, D), $I_{L,Ca}$ started to appear at Vm = -30 mV, reached maximum at around $V_m$ = +10 mV, and decreased at higher voltages approaching zero at about $V_m$ = +60 mV (Fig. 6D). Maximal amplitudes of $I_{L,Ca}$ were suppressed in the presence of CBD (1 μM).

CBD did not change the steady-state activation curve of $I_{L,Ca}$ ($V_{1/2}$ values in control and in the presence of CBD are -19.1 ± 0.4 mV and -17.6 ± 0.3 mV, respectively; n=6, paired *t*-test, P>0.05) (Fig.7A). However, there was a hyperpolarizing shift of $I_{L,Ca}$ steady-state inactivation by 9.6 mV (i.e., from control value $V_{1/2}$= -10.2 ± 0.9 mV to $V_{1/2}$= -19.8 ± 1.1 mV in the presence of CBD) (Fig 7B). However, there was little influence on the slopes of respective curves (k = 7.7 ± 0.5 mV and k = -4.5 ± 0.4 mV for the control activation and inactivation, respectively, vs. k = 7.9 ± 0.3 mV and k = -4.2 ± 0.3 mV for the CBD-modified activation and inactivation, respectively).

In line with earlier reports [22], kinetic analysis of $I_{L,Ca}$ currents were fit to double-exponential function with fast ($\tau_f$) and slow ($\tau_s$) inactivation time constants. Comparison of $I_{L,Ca}$ currents in the absence and presence of CBD revealed noticeable acceleration of the current's inactivation kinetics by CBD. Quantification of the time constants of $I_{L,Ca}$ inactivation showed that CBD (1 μM) significantly reduced $\tau_i$ in the range of $V_m$ -30 mV and +10 mV (Fig. 7C).

*Effects of CBD on [$^3$H]Isradipine binding*

It was possible that CBD interacts directly with the binding site of dihydropyridine class of $Ca^{2+}$ channel antagonists on L-type $Ca^{2+}$ channels. For this reason, we tested the effect of CBD on the specific binding of [$^3$H]Isradipine. Equilibrium curves for the binding of [$^3$H]Isradipine, in the presence and absence of the CBD are presented in Figure 8A (n= 9-11). At a concentration of 10 μM, CBD did not cause a significant inhibition of the specific binding of [$^3$H]Isradipine. In controls and in presence of 10 μM CBD, maximum binding activities (Bmax) were 196 ± 12 and 184 ± 9 fM/mg protein, and $K_D$ values were 98 ± 11 and 92 ± 8 pM, respectively. There was no statistically significant difference between control and CBD treated groups with respect to Bmax values ($P$>0.05, ANOVA, n=9-11). The effect of increasing CBD concentration was also investigated on the specific [$^3$H]Isradipine binding from cardiac muscle membranes (Fig. 7C). In the concentration range used (0.1 to 30 μM), CBD did not alter the specific binding of [$^3$H]Isradipine.

**Discussion**

The results of this study indicate for the first time that inhibition of $Ca^{2+}$ signaling underlies the negative inotropic actions of CBD in rat ventricular myocytes and that the inhibition of L-type $Ca^{2+}$ channel mediates the effects of CBD on myocyte contractility.

Administration of cannabinoids, such as THC and CBD, causes complex hemodynamic changes involving phases of both increased and decreased blood pressure as well as changes in heart rate and contractility [for reviews, 10, 23]. CBD has been shown to have various effects on muscular structures, neuronal and endothelial cells and alter the activities of several receptors, ion channels [for reviews, 3, 9, 24] and neurotransmitter transporters [24, 25]. However, using video edge detection system allows measurement of contractility at single-cell level in a relatively isolated environment and excludes the influence of autonomic nerve endings, gap-junctions, neurotransmitter uptake system, and coronary perfusion status. In our experiments, CBD caused a significant reduction in the maximal shortening amplitudes without significantly altering the time course of myocyte contraction. These findings provide evidence that the negative inotropic effect of CBD reported in earlier studies [14, 15] results from a direct interaction of CBD with ventricular myocytes, rather than actions of CBD on nerve endings and neurotransmitter uptake systems in the heart.

CBD has been shown to have antagonist effects on GPR55 [27]. Therefore antagonism of a constitutive GPR55 activity can mimic the actions of CBD on the contractility of cardiomyocytes. However, AM251, an agonist of GPR55 and antagonist/inverse agonist of CB1 receptor, does not alter the contractility of cardiomyocytes and amplitudes of L-type $Ca^{2+}$ currents [28, 29] suggesting that antagonism of GPR55 receptors does not mediate the effects of CBD in cardiomyocytes. In several recent studies, activation of peroxisome proliferator-activated receptor gamma (PPARγ) has been shown to mediate the effects of CBD [13, 30]. However, PPARγ antagonist, GW9662 (1 μM, [13]), did not reverse the effects of CBD on myocyte shortening (data not shown).

Negative inotropic actions of CBD might be attributed to the inhibition of $Ca^{2+}$ release from the SR. In fact, CBD and other cannabinoids have been reported to modulate the ryanodine sensitive intracellular $Ca^{2+}$ stores in neurons [9, 31]. However, the amplitude and kinetics of caffeine-induced $Ca^{2+}$ release from intracellular $Ca^{2+}$ stores were not changed by CBD suggesting that ryanodine-sensitive intracellular $Ca^{2+}$ stores are not involved in negative inotropic effects of CBD observed in this study. CBD can alter the levels of second messengers such as cAMP, cGMP and protein kinase C which are known to be involved in tuning the $Ca^{2+}$ sensitivity of the contractile proteins. In an earlier study in cardiac muscle membranes, cAMP levels have been shown to be unaltered in the presence of CBD [32]. Furthermore, sensitivity of contractile proteins to intracellular $Ca^{2+}$ remained unchanged in the presence of CBD suggesting that phosphorylation and de-phosphorylation of the contractile proteins do not play a significant role in negative inotropic actions of CBD. Collectively, these results suggest that the effects of CBD on myocyte contractility are not related to changes in intracellular $Ca^{2+}$ release machinery or sensitivity of myofilaments to $Ca^{2+}$. In addition, in the presence of CBD, resting levels of intracellular $Ca^{2+}$ and cell length of ventricular myocytes remained unaltered suggesting that CBD does not significantly affect $Ca^{2+}$ homeostasis under resting conditions.

During excitation-contraction coupling, alterations in the amplitudes and kinetics of cardiac AP are closely associated with corresponding changes in the contractility of myocytes [33]. In our study, CBD decreased durations of APs without significantly affecting the amplitudes and $dV/dt_{max}$ of APs suggesting that voltage-gated sodium channels are not affected by CBD. In cardiac muscle, extracellular $Ca^{2+}$ required to trigger $Ca^{2+}$ release from SR enters through L-type voltage-dependent $Ca^{2+}$ channels opened during the AP. Results of whole-cell patch clamp experiments indicate that, in line with the decrease of AP duration, CBD (1-10 μM) caused a significant inhibition of voltage-dependent L-type $Ca^{2+}$ channels in cardiomyocytes by accelerating the inactivation of these channels.

Left-ward (hyperpolarizing) shift of the inactivation curve, together with increased acceleration of inactivation kinetics, indicate that more L-type $Ca^{2+}$ channels would be in closed state during action potential. Inactivation of these channels would cause shortening of action potential since the L-type $Ca^{2+}$ channels are the main conductance during plateau phase (phase 2) of the ventricular action potential. Collectively, these results suggest that during excitation-contraction coupling, shortening of action potential due to the inhibition of L-type $Ca^{2+}$ channels decreases $Ca^{2+}$-induced $Ca^{2+}$ release from SR and causes negative inotropic effect of CBD reported in earlier studies. In line with this hypothesis, although caffeine-induced contractures and myofilament sensitivity to $Ca^{2+}$ remained unchanged, electrically-induced $Ca^{2+}$ transients were significantly depressed by CBD; further suggesting that $Ca^{2+}$-induced $Ca^{2+}$ release was inhibited in the presence of CBD.

In clinical studies, acute CBD intake does not cause a significant change in blood pressure and heart rate [for a review, 10]. However, several earlier studies indicate that the increases in blood pressure and heart rate during stressful conditions are markedly attenuated by CBD [34, 35, 36]. In *in vivo* studies, increased heart rate and blood pressure, two of the most consistent effects of *Cannabis* intoxication, are also decreased by CBD [15]. Collectively these results suggest that CBD, at relatively high concentrations, can suppress the function of cardiovascular system. In fact, cardiac failure due to depressed heart contractility has been suggested to be the main cause of mortality in *Cannabis* intoxication [for a review, 37]. Thus it is likely that some of the effects of *Cannabis* plant are mediated by CBD during *Cannabis* intoxication.

In addition to cardiac contractility, the electrical activity of the heart has also been suggested to be affected by CBD. In an earlier study, CBD has been shown to have beneficial actions in ischemia-induced cardiac arrhythmias [6]. Shortening of AP duration by CBD observed in our study can be beneficial or harmful, depending on the underlying pathology. Thus, during acute ischemia, in which

the duration of the cardiac APD is already shortened, a further decrease should be proarrhythmic [for a review, 38]. However, shortening of AP duration may be beneficial in preventing those arrhythmias caused by triggered activities observed in conditions such as heart failure [38]. In conclusion, the results indicate for the first time that CBD inhibits myocyte contractility by acting on L-type $Ca^{2+}$ channels.

**Acknowledgments**

This study was in part supported by the NIDA/NIH, USA and the United Arab Emirates University Research Funds. Research in our laboratory is also supported by LABCO partner of Sigma-Aldrich.

**Conflict of Interest:** None

**Author contributions:** Ramez M. Ali, Lina T. Al Kury, Anwar Qureshi: conducted experiments. Keun-Hang Susan Yang, Mohanraj Rajesh, Sehamuddin Galadari: design of the experiments, Yaroslav M. Shuba, Frank Christopher Howarth, Murat Oz: analysis of data and the writing of the paper.

Reference List

[1] Izzo AA, Borrelli F, Capasso R, Di M, V and Mechoulam R (2009) Non-psychotropic plant cannabinoids: new therapeutic opportunities from an ancient herb. *Trends Pharmacol Sci* 30:515-527.

[2] Booz GW (2011) Cannabidiol as an emergent therapeutic strategy for lessening the impact of inflammation on oxidative stress. *Free Radic Biol Med* 51:1054-1061.

[3] Pertwee RG (2008) The diverse CB1 and CB2 receptor pharmacology of three plant cannabinoids: delta9-tetrahydrocannabinol, cannabidiol and delta9-tetrahydrocannabivarin. *Br J Pharmacol* 153:199-215.

[4] De Petrocellis L and Di Marzo, V (2010) Non-CB1, non-CB2 receptors for endocannabinoids, plant cannabinoids, and synthetic cannabimimetics: focus on G-protein-coupled receptors and transient receptor potential channels. *J Neuroimmune Pharmacol* 5:103-121.

[5] Durst R, Danenberg H, Gallily R, Mechoulam R, Meir K, Grad E, et al., (2007) Cannabidiol, a nonpsychoactive Cannabis constituent, protects against myocardial ischemic reperfusion injury. Am J Physiol Heart Circ Physiol 293:H3602-H3607.

[6] Walsh SK, Hepburn CY, Kane KA and Wainwright CL (2010) Acute administration of cannabidiol in vivo suppresses ischaemia-induced cardiac arrhythmias and reduces infarct size when given at reperfusion. Br J Pharmacol 160:1234-1242.

[7] Rajesh M, Mukhopadhyay P, Batkai S, Patel V, Saito K, Matsumoto S, et al., (2010) Cannabidiol attenuates cardiac dysfunction, oxidative stress, fibrosis, and inflammatory and cell death signaling pathways in diabetic cardiomyopathy. J Am Coll Cardiol 56:2115-2125.

[8] Fouad AA, Albuali WH, Al-Mulhim AS and Jresat I (2013) Cardioprotective effect of cannabidiol in rats exposed to doxorubicin toxicity. *Environ Toxicol Pharmacol* 36:347-357.

[9] Pertwee RG, Howlett AC, Abood ME, Alexander SP, Di M, V, Elphick MR, et al., (2010) International Union of Basic and Clinical Pharmacology. LXXIX. Cannabinoid receptors and their ligands: beyond CB and CB. Pharmacol Rev 62:588-631.

[10] Stanley CP, Hind WH and O'Sullivan SE (2013a) Is the cardiovascular system a therapeutic target for cannabidiol? *Br J Clin Pharmacol* 75:313-322.

[11] Offertaler L, Mo FM, Batkai S, Liu J, Begg M, Razdan RK, et al., (2003) Selective ligands and cellular effectors of a G protein-coupled endothelial cannabinoid receptor. *Mol Pharmacol* 63:699-705.

[12] Stanley CP, Wheal AJ, Randall MD and O'Sullivan SE (2013b) Cannabinoids alter endothelial function in the Zucker rat model of type 2 diabetes. *Eur J Pharmacol* 720:376-382.

[13] O'Sullivan SE, Sun Y, Bennett AJ, Randall MD and Kendall DA (2009) Time-dependent vascular actions of cannabidiol in the rat aorta. *Eur J Pharmacol* 612:61-68.

[14] Smiley KA, Karler R and Turkanis SA (1976) Effects of cannabinoids on the perfused rat heart. Res Commun Chem Pathol Pharmacol 14:659-675.

[15] Nahas G and Trouve R (1985) Effects and interactions of natural cannabinoids on the isolated heart. Proc Soc Exp Biol Med 180:312-316.

[16] Howarth FC, Qureshi MA and White E (2002) Effects of hyperosmotic shrinking on ventricular myocyte shortening and intracellular Ca(2+) in streptozotocin-induced diabetic rats. *Pflugers Arch* 444:446-451.

[17] Howarth FC and Qureshi MA (2006) Effects of carbenoxolone on heart rhythm, contractility and intracellular calcium in streptozotocin-induced diabetic rat. *Mol Cell Biochem* 289:21-29.

[18] Bassani JW, Yuan W and Bers DM (1995) Fractional SR Ca release is regulated by trigger Ca and SR Ca content in cardiac myocytes. *Am J Physiol* 268:C1313-C1319.

[19] Spurgeon HA, duBell WH, Stern MD, Sollott SJ, Ziman BD, Silverman HS, et al., (1992) Cytosolic calcium and myofilaments in single rat cardiac myocytes achieve a dynamic equilibrium during twitch relaxation. J Physiol 447:83-102.:83-102.

[20] Oz M, Tchugunova Y and Dinc M (2004) Differential effects of endogenous and synthetic cannabinoids on voltage-dependent calcium fluxes in rabbit T-tubule membranes: comparison with fatty acids. *Eur J Pharmacol* 502:47-58.

[21] Voitychuk OI, Asmolkova VS, Gula NM, Sotkis GV, Galadari S, Howarth FC, et al., (2012) Modulation of excitability, membrane currents and survival of cardiac myocytes by N-acylethanolamines. *Biochim Biophys Acta* 1821:1167-1176.

[22] Soldatov NM, Oz M, O'Brien KA, Abernethy DR and Morad M (1998) Molecular determinants of L-type Ca2+ channel inactivation. Segment exchange analysis of the carboxyl-terminal cytoplasmic motif encoded by exons 40-42 of the human alpha1C subunit gene. J Biol Chem 273:957-963.

[23] Malinowska B, Baranowska-Kuczko M and Schlicker E (2012) Triphasic blood pressure responses to cannabinoids: do we understand the mechanism? *Br J Pharmacol* 165:2073-2088.

[24] Oz M (2006) Receptor-independent actions of cannabinoids on cell membranes: focus on endocannabinoids. *Pharmacol Ther* 111:114-144.

[25] Poddar MK and Dewey WL (1980) Effects of cannabinoids on catecholamine uptake and release in hypothalamic and striatal synaptosomes. *J Pharmacol Exp Ther* 214:63-67.

[26] Pandolfo P, Silveirinha V, dos Santos-Rodrigues A, Venance L, Ledent C, Takahashi RN, et al., (2011) Cannabinoids inhibit the synaptic uptake of adenosine and dopamine in the rat and mouse striatum. *Eur J Pharmacol* 655:38-45.

[27] Sharir H, Abood ME. (2010) Pharmacological characterization of GPR55, a putative cannabinoid receptor. Pharmacol Ther. 126: 301-313.

[28] Al Kury LT, Voitychuk OI, Ali RM, Galadari S, Yang KH, Howarth FC, et al.,. (2014a) Effects of endogenous cannabinoid anandamide on excitation-contraction coupling in rat ventricular myocytes. Cell Calcium. 55: 104-118.

[29] Al Kury LT, Voitychuk OI, Yang KH, Thayyullathil FT, Doroshenko P, Ramez AM, et al., (2014b) Effects of the endogenous cannabinoid anandamide on voltage-dependent sodium and calcium channels in rat ventricular myocytes. Br J Pharmacol. 171: 3485-3498.

[30] O'Sullivan SE, Kendall DA. (2010) Cannabinoid activation of peroxisome proliferator-activated receptors: potential for modulation of inflammatory disease. Immunobiology. 215:611-616.

[31] Drysdale AJ, Ryan D, Pertwee RG and Platt B (2006) Cannabidiol-induced intracellular Ca2+ elevations in hippocampal cells. *Neuropharmacology* 50:621-631.

[32] Hillard CJ, Pounds JJ, Boyer DR and Bloom AS (1990) Studies of the role of membrane lipid order in the effects of delta 9-tetrahydrocannabinol on adenylate cyclase activation in heart. *J Pharmacol Exp Ther* 252:1075-1082.

[33] Sah R, Ramirez RJ, Oudit GY, Gidrewicz D, Trivieri MG, Zobel C, et al., (2003) Regulation of cardiac excitation-contraction coupling by action potential repolarization: role of the transient outward potassium current (I(to)). J Physiol. 546:5-18.

[34] Resstel LB, Joca SR, Moreira FA, Correa FM and Guimaraes FS (2006) Effects of cannabidiol and diazepam on behavioral and cardiovascular responses induced by contextual conditioned fear in rats. Behav Brain Res 172:294-298.

[35] Resstel LB, Tavares RF, Lisboa SF, Joca SR, Correa FM and Guimaraes FS (2009) 5-HT1A receptors are involved in the cannabidiol-induced attenuation of behavioural and cardiovascular responses to acute restraint stress in rats. Br J Pharmacol 156:181-188.

[36] Gomes FV, Alves FH, Guimaraes FS, Correa FM, Resstel LB and Crestani CC (2013) Cannabidiol administration into the bed nucleus of the stria terminalis alters cardiovascular responses induced by acute restraint stress through 5-HT(1)A receptor. Eur Neuropsychopharmacol 23:1096-1104.

[37] Bergamaschi MM, Queiroz RH, Zuardi AW and Crippa JA (2011) Safety and side effects of cannabidiol, a Cannabis sativa constituent. *Curr Drug Saf* 6:237-249.

[38] Den Ruijter HM, Berecki G, Opthof T, Verkerk AO, Zock PL and Coronel R (2007) Pro- and antiarrhythmic properties of a diet rich in fish oil. *Cardiovasc Res* 73:316-325.

**FIGURE LEGENDS**

**Figure 1: Effects of CBD on ventricular myocyte shortening. (A)** Typical records of shortening in an electrically stimulated (1 Hz) ventricular myocyte superfused with either NT (containing the vehicle, 0.02% DMSO) or NT + 1 μM CBD and during washout with NT. **(B)** Time course of the mean amplitudes (AMP) of shortening expressed as a percentage of control values in vehicle (NT + 0.02% DMSO), and in presence of CBD (1 μM). Myocytes were maintained at 35-36 °C and superfused with CBD for 10 min. Data are shown as means ± S.E.M., n = 6-8 cells. **(C)** Bar graph showing the mean amplitudes (AMP) of shortening expressed as a percentage of control values in the presence of vehicle, and in presence of CBD after 10 min bath exposure to CBD (1 μM). Data are shown as means ± S.E.M., n = 17 cells. * indicates statistically significant difference at the level of $P < 0.05$. **(D)** Concentration-response curve for the inhibitory effect of CBD on myocyte shortening. The data was normalized to the maximal inhibitory effect of CBD and plotted as a function of CBD concentrations. Each data point represents means ± S.E.M. from n = 6-8 cells for each concentration.

**Figure 2: Effects of CBD on amplitude and time-course of intracellular $Ca^{2+}$ in rat ventricular myocytes. (A)** Typical records of $Ca^{2+}$ transients in an electrically stimulated (1 Hz) ventricular myocyte superfused with either NT or NT + 1 μM CBD and during washout with NT; scale bar indicates 0.1 fura-2 ratio unit (RU). Also shown resting fura-2 ratio (340/380 nm) (**B**), time to peak (TPK) $Ca^{2+}$ transient **(C)**, time to half ($T_{HALF}$) decay of the $Ca^{2+}$ transients **(D)** and amplitude (AMP) of the $Ca^{2+}$ transients **(E)**. Myocytes were maintained at 35-36 °C and superfused with CBD for 10 min. Data are shown as means ± SEM, n=11-14 cell. * indicates statistically significant difference at the level of $P < 0.05$.

**Figure 3: Effects of CBD on sarcoplasmic reticulum $Ca^{2+}$ transport. (A)** Typical records illustrating the effects of CBD on caffeine-induced $Ca^{2+}$ transients. **(B)** Comparison of the effect of caffeine application on the area under caffeine-evoked $Ca^{2+}$ transients in NT and CBD-treated cells in rat ventricular myocytes. **(C)** Typical record illustrating the effects of electrical stimulation (ES) and rapid application of caffeine on fura-2 ratio. **(D)** Mean amplitude of SR fractional release of $Ca^{2+}$ (on the right) and recovery of electrically evoked intracellular $Ca^{2+}$ after application of caffeine (on the left). Data are shown as means ± S.E.M., n = 7-8 cells.

**Figure 4: Effects of CBD on myofilament sensitivity to $Ca^{2+}$. (A)** Typical record of myocyte shortening and fura-2 ratio and phase-plane diagrams of fura-2 ratio vs. cell length in a myocytes exposed to NT. The arrow indicates the region where the gradient was measured. **B-D** show the effect of 1 μM CBD on the mean gradient of the fura-2 cell length trajectory of the twitch contraction during the periods 500-600 **(B)**, 500-700 **(C)** and 500-800 ms **(D)** of late relaxation. Data are shown as means ± S.E.M., n = 17 cells.

**Figure 5: Effects of CBD on the action potentials of ventricular myocytes. (A)** Representative recordings show the APs in controls (dark grey area), in the presence of 1 μM CBD (light grey area) and after washout (striped area) in the ventricular myocytes; the *insets* on panel A show the time course of the action potential duration ($APD_{60}$) and resting potential ($V_{rest}$) changes in response to CBD application (indicated by horizontal bars). **(B-E)** show summary of CBD effects on amplitude and shape of the AP in cardiomyocytes; quantification of the changes in $V_{rest}$ **(B)**, AP amplitude **(C)**, AP maximal rate of rise **(D)** and AP duration (**E)**, characterized by $APD_{60}$ in controls (*dark grey bars*) and in response to 1 μM CBD (*light grey bars*). Data are shown as means ± S.E.M. from 6 to 9 myocytes for each group.

**Figure 6: Effects of cannabidiol on $Ca^{2+}$ currents mediated by L-type $Ca^{2+}$ channels in rat ventricular myocytes. (A)** CBD inhibits L-type $Ca^{2+}$ currents recorded using whole-cell voltage-clamp mode of patch clamp technique. Current traces are recorded before (control) and after 10 min application of 1 μM CBD. L-type $Ca^{2+}$ currents were recorded during 300 ms voltage pulses to +10 mV from a holding potential of -50 mV. **(B)** Averages of the maximal currents of VGCCs presented as a function of time in the presence of vehicle (0.02% DMSO; filled circles) and 1 μM CBD (n=5 cells; open circles). Application time for the agents was presented in horizontal bars. **(C)** Representative recordings of $I_{Ca}$ in response to the depicted pulse protocol under control conditions and after application of 1μM CBD**. (D)** Normalized and averaged *I-V* relationships of control $I_{Ca}$ (filled circles) and $I_{Ca}$ in the presence of 1 μM CBD (open circles) determined by applying a series of step depolarizing pulses from -70 mV to +70 mV in 10 mV increments for a duration of 300 ms. Data points (means ± S.E.M.) are from 5 to 7 cells.

**Figure 7: Effects of CBD on steady state activation and inactivation of $I_{Ca}$ in rat ventricular myocytes.** Steady-state activation (SSA) **(A)** and steady-state inactivation (SSI) **(B)** curves of $I_{Ca}$ in the absence (filled circles) and presence of 1 μM CBD (open circles). Data points (mean ± S.E.M.) are from 5 cells. Fit of experimental data points with Boltzmann equation. **(C)** Voltage-dependent fast (triangles) and slow (circles) inactivation time constants (τi) of $I_{L,Ca}$ under control conditions (filled circles, and triangles) and in the presence of 1 μM CBD (open circles and triangles). Data points (means ± S.E.M.) are from 5-6 cells.

**Fig. 8: Effects of CBD on the specific binding of [$^3$H]Isradipine to rat ventricular muscle membranes**. **(A)** Specific binding as a function of the concentration of [$^3$H]Isradipine in the absence and presence of CBD. Data points for controls and CBD (1 μM) are indicated by filled and open circles, respectively. **(B)** Effects of increasing the concentration of CBD on the specific binding of [$^3$H]Isradipine to cardiac muscle membranes. Data are the means± S.E.M. of 9-11 experiments.

- Highlights

- The effects of CBD on contractility and electrophysiological properties of rat ventricular myocytes were investigated using video edge detection, the Ca2+ sensitive fluorescent indicator fura-2 AM, whole-cell patch clamp, and radioligand binding methods.

- CBD caused a significant decrease in the amplitudes of electrically-evoked myocyte shortening and Ca2+ transients and inhibited L-type Ca2+ channels.

- The results suggest that CBD depresses myocyte contractility by suppressing L-type Ca2+ channels at a site different than dihydropyridine binding site and inhibits excitation-contraction coupling in cardiomyocytes.

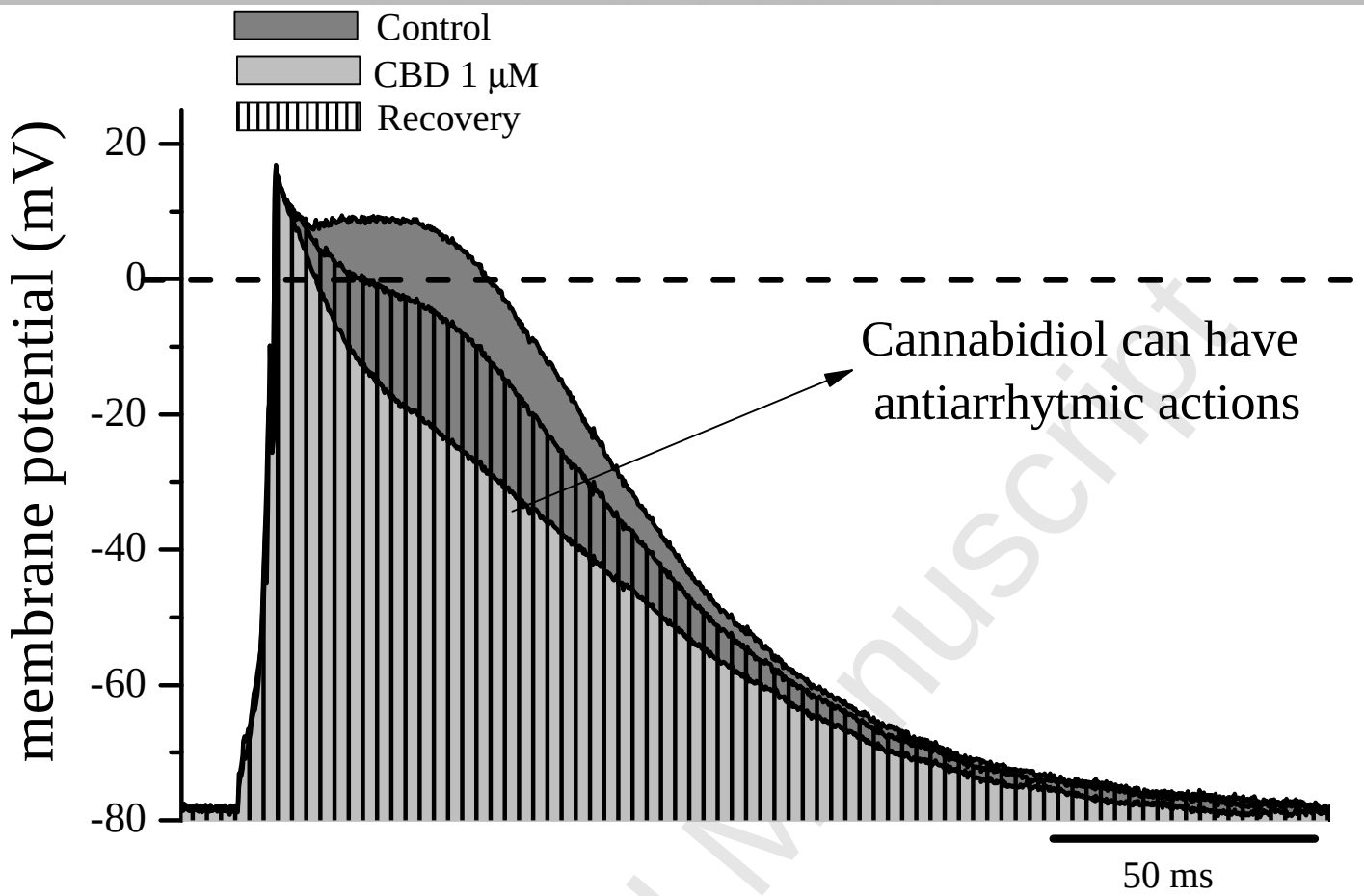

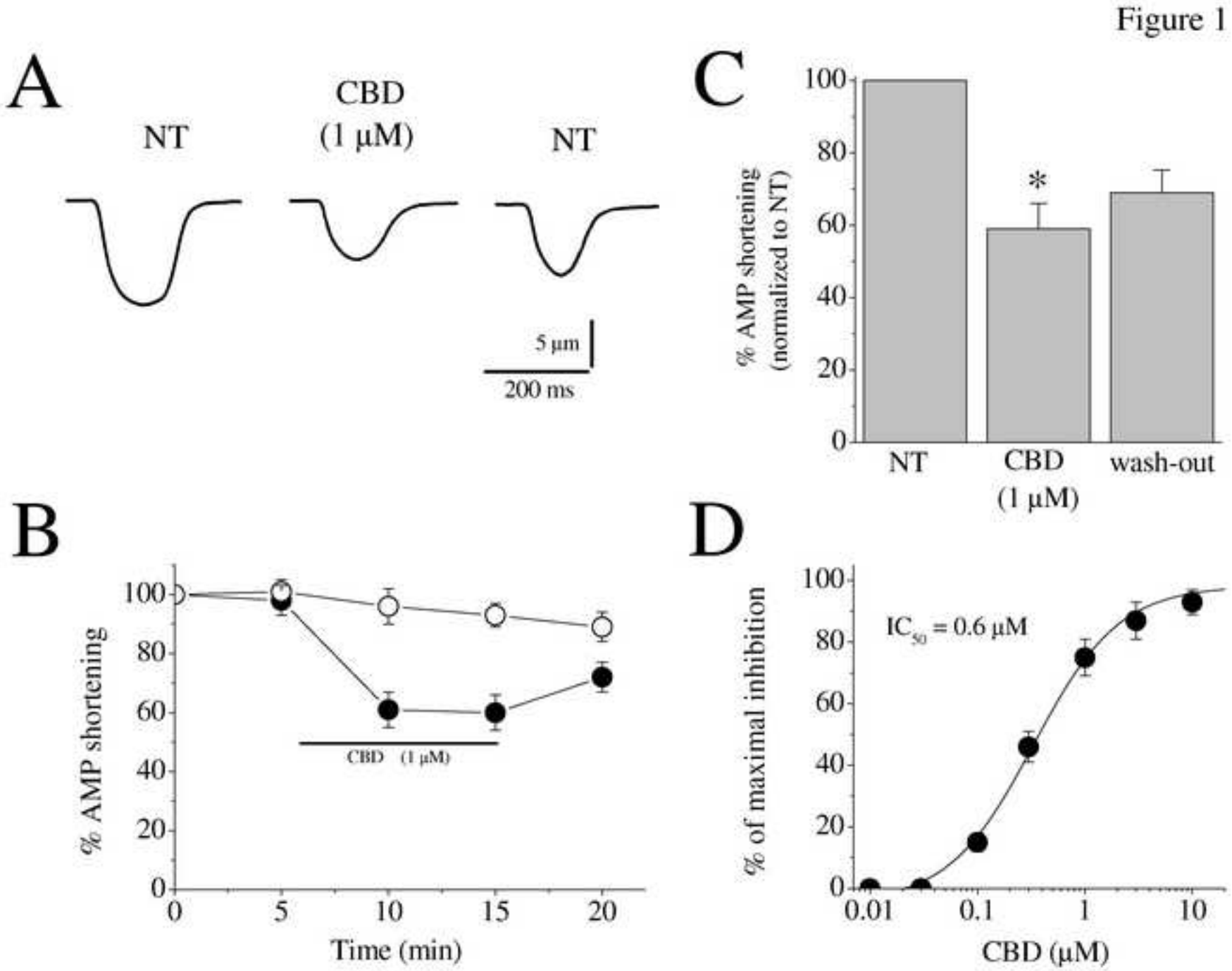
Figure 1
A
NT
CBD
(1 µM)
NT
5 µm
200 ms
C
% AMP shortening
(normalized to NT)
100
80
60
40
20
0
*
NT
CBD
(1 µM)
wash-out
B
% AMP shortening
100
80
60
40
20
0
CBD (1 µM)
0
5
10
15
20
Time (min)
D
% of maximal inhibition
IC50 = 0.6 µM
100
80
60
40
20
0
0.01
0.1
1
10
CBD (µM)

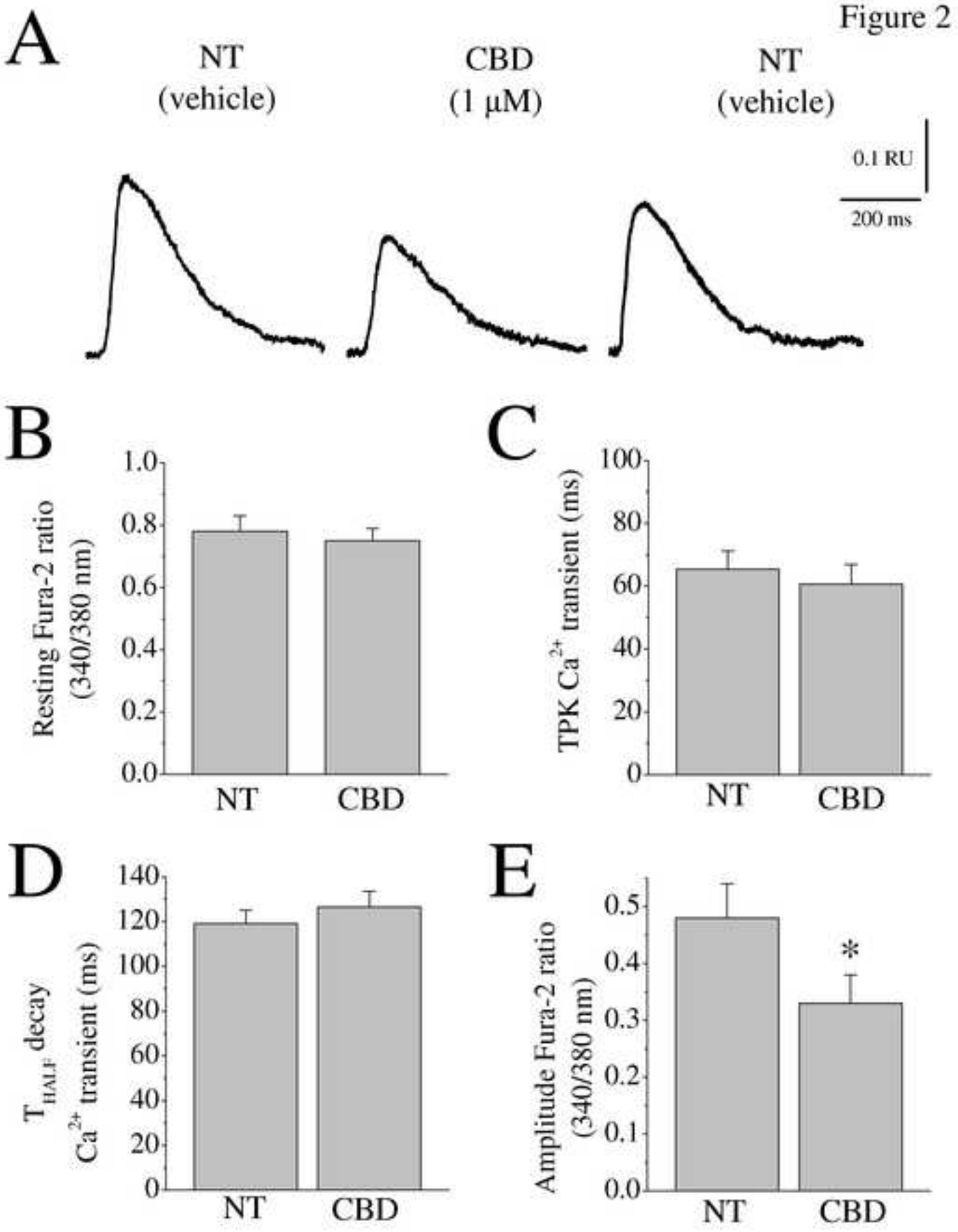

**Figure3**

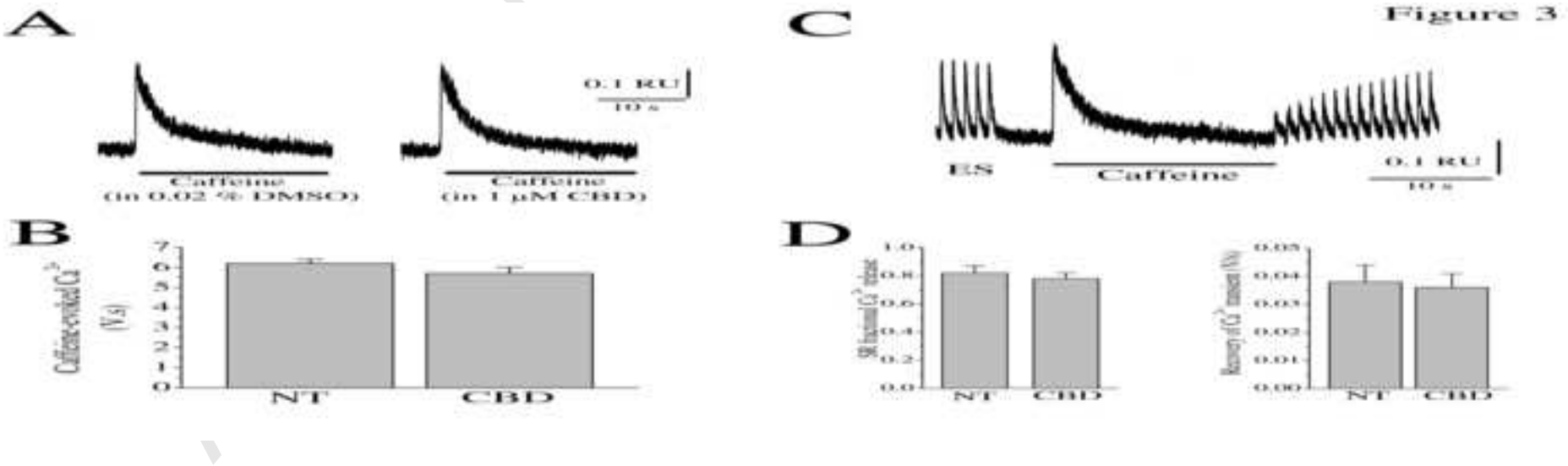


Figure 3

Figure 4

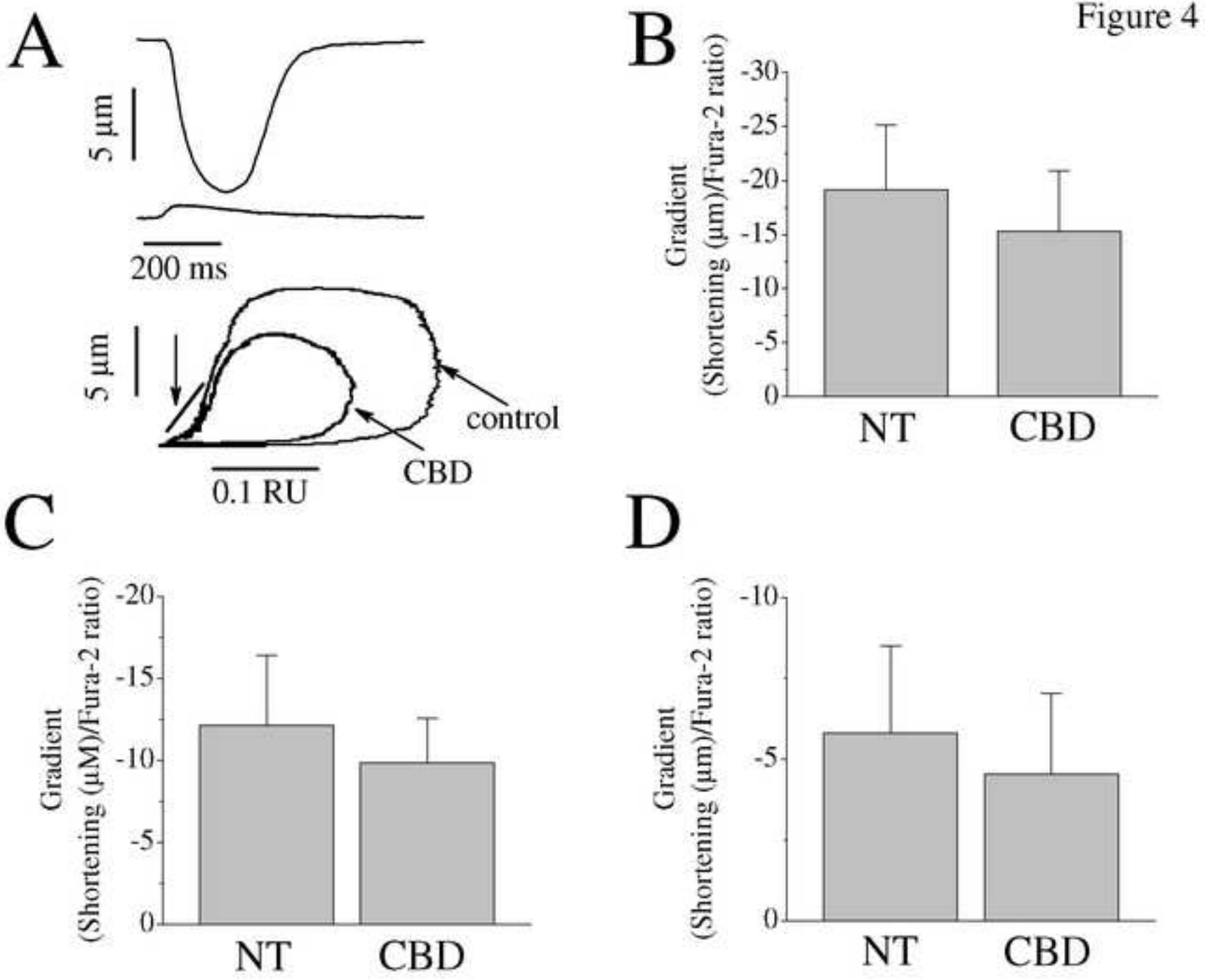
A
5 µm
200 ms
5 µm
control
CBD
0.1 RU
B
Gradient
(Shortening (µm)/Fura-2 ratio)
-30
-25
-20
-15
-10
-5
0
NT
CBD
C
Gradient
(Shortening (µM)/Fura-2 ratio)
-20
-15
-10
-5
0
NT
CBD
D
Gradient
(Shortening (µm)/Fura-2 ratio)
-10
-5
0
NT
CBD

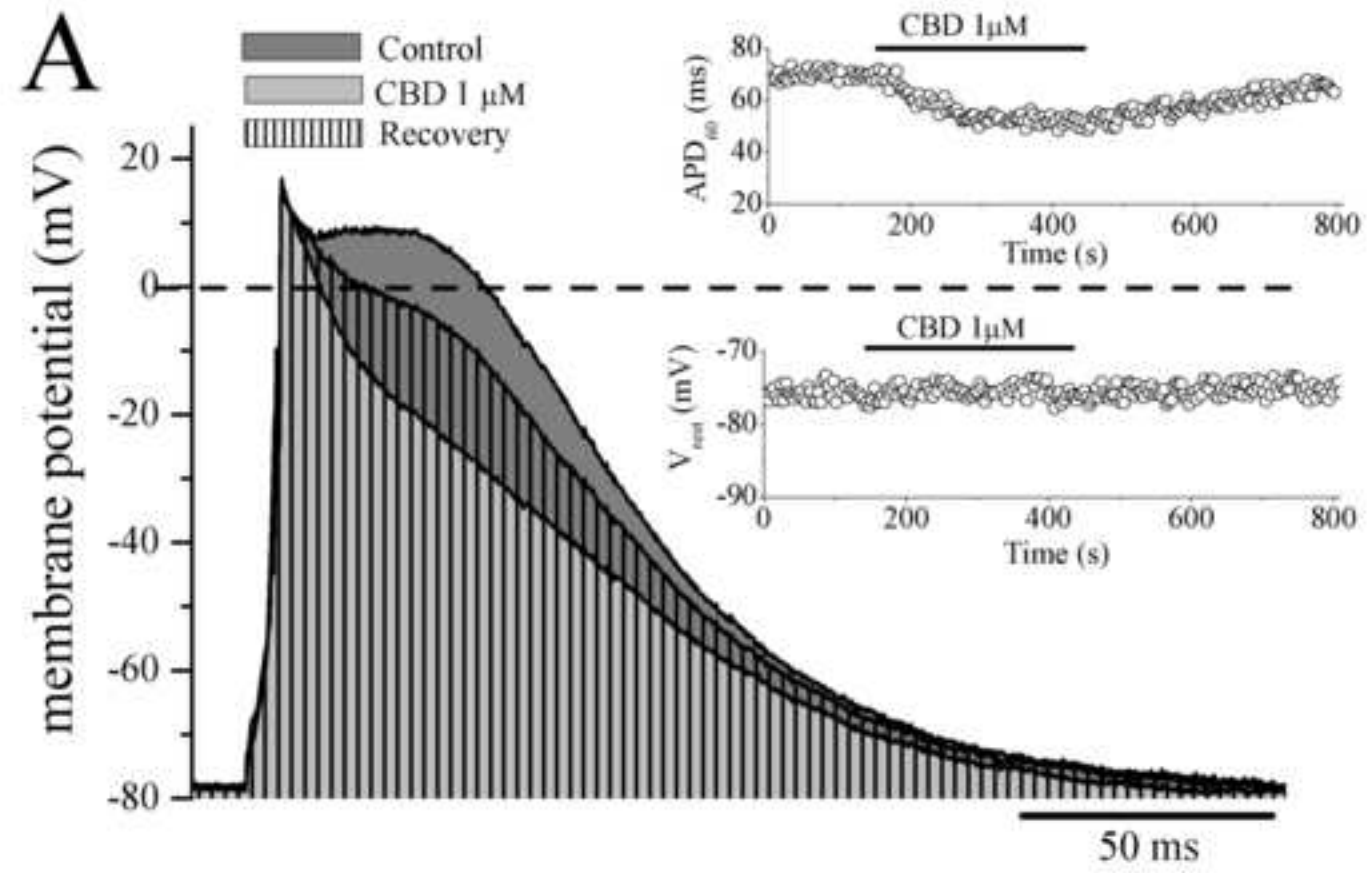


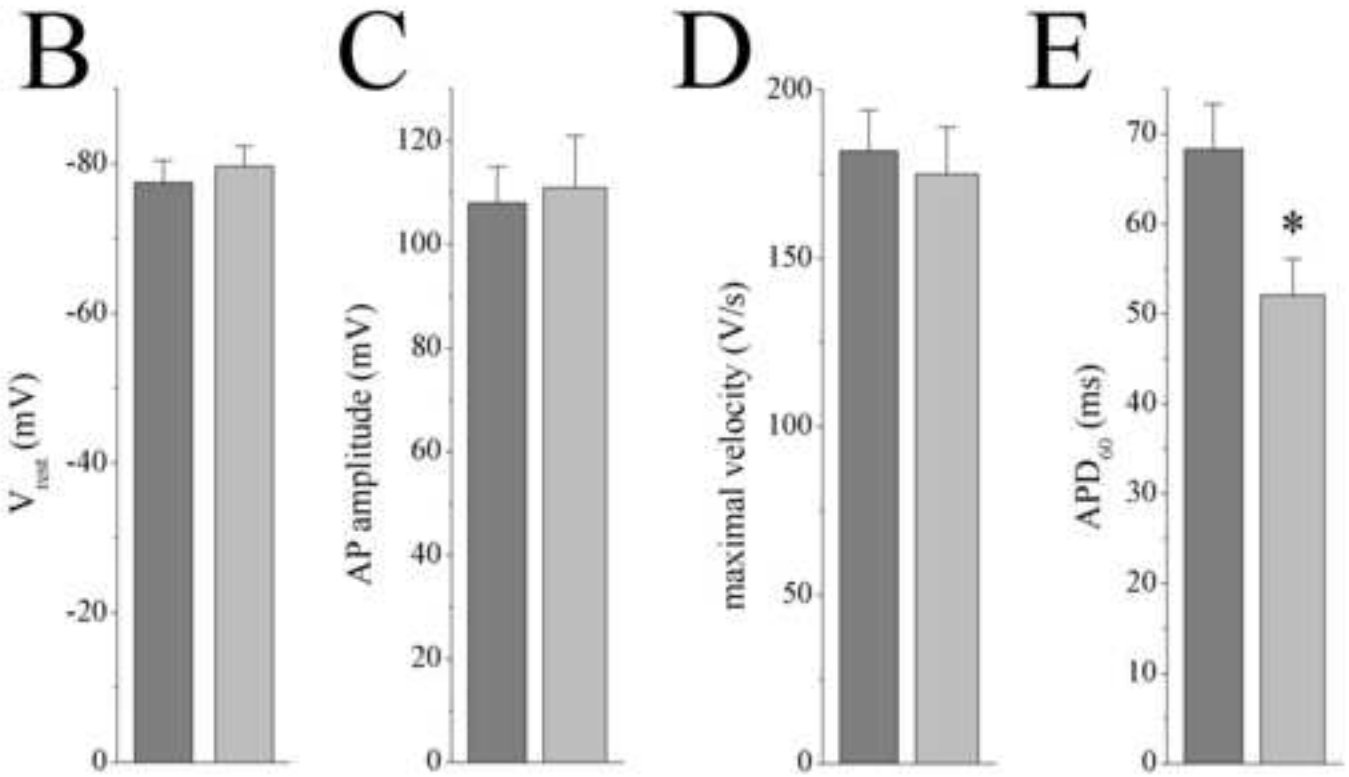


Figure 5

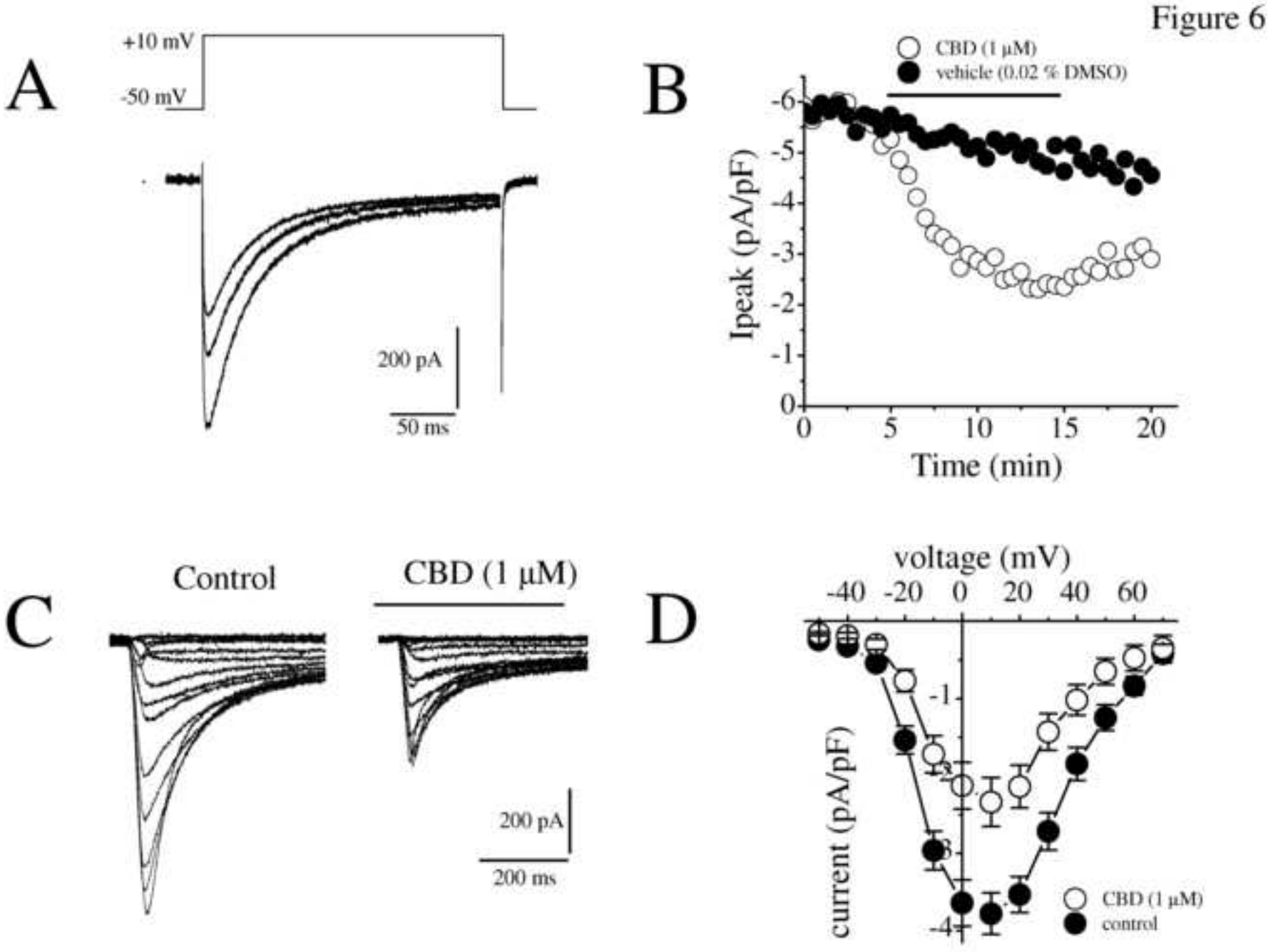
Figure 6
A
+10 mV
-50 mV
200 pA
50 ms
B
CBD (1 μM)
vehicle (0.02 % DMSO)
Ipeak (pA/pF)
Time (min)
C
Control
CBD (1 μM)
200 pA
200 ms
D
voltage (mV)
current (pA/pF)
CBD (1 μM)
control

Figure 7

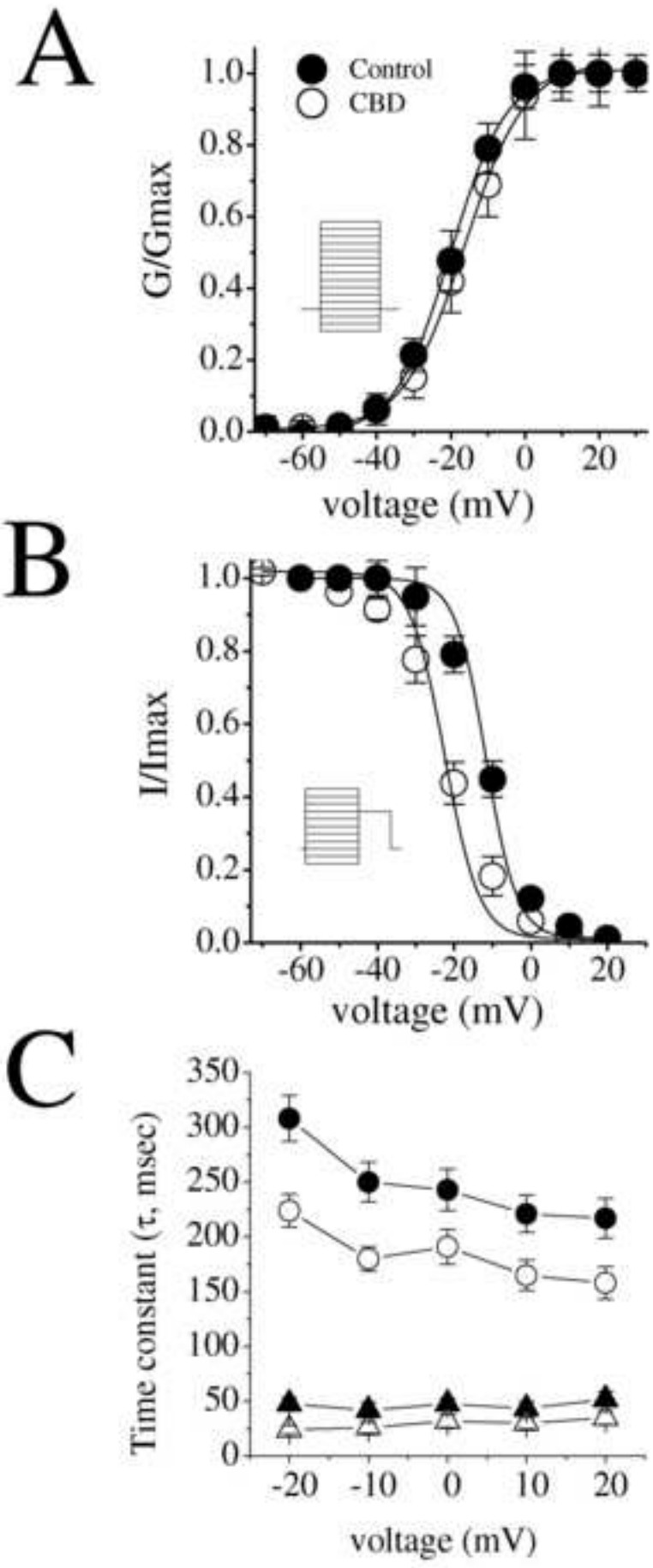

Figure 8